

8th International Congress on Catalysis

Proceedings

Vol. 5

8th International Congress on Catalysis

Volume V: Cluster-derived catalysts
Active phase-support interactions
Catalysis for synthesis of chemicals



Weinheim
Deerfield Beach, Florida
Basel



Responsible for the contents: **The Authors**

(Their ready-for-copy manuscripts have been printed without corrections)

Allrights reserved

© 1984 by DECHEMA, Deutsche Gesellschaft für chemisches Apparatewesen e.V.
Frankfurt am Main

Printed: Schön & Wetzel GmbH, Frankfurt am Main

ISBN 3-527-26232-6 (Weinheim, Basel)

ISBN 0-89573-376-5 (Deerfield Beach)

CONTENTS

Cluster — derived catalysts

V. L. Kuznetsov, A. V. Romanenko, I. L. Mudrakovskii, V. M. Mastikhin, Yu. I. Yermakov, V. A. Shmachkov, Novosibirsk/USSR Study of supported rhodium catalysts for synthesis of low alcohols from CO and H ₂	3— 14	42
K. Kaneda, T. Imanaka, S. Teranishi, Osaka/J Rhodium cluster catalysis in hydrogenation and carbonylation of olefins using carbon monoxide and water	15— 26	42
D. J. Hunt, R. B. Moyes, P. B. Wells, S. D. Jackson, R. Whyman, Hull and Runcorn/UK Catalysis by supported metal clusters derived from H ₄ Os ₄ (CO) ₁₂	27— 38	42
J. F. Knifton, Austin TX/USA The selective preparation of ethylene glycol, alkanols and acetic acid directly from synthesis gas	39— 50	42
R. Nakamura, A. Oomura, E. Echigoya, Tokyo/J The chemistry and catalysis of Co ₂ (CO) ₈ /oxides	51— 62	42
T. Beringhelli, A. Gervasini, F. Morazzoni, D. Strumolo, S. Martinengo, L. Zanderighi, F. Pinna, G. Strukul, Milano and Venezia/I Highly dispersed Rh on γ -Al ₂ O ₃ , ZrO ₂ , TiO ₂ : morphological and electronic characterization	63— 73	42
P. G. Gopal, K. L. Watters, Milwaukee WI/USA A study of cobalt carbonyls deposited on magnesia	75— 85	43
O. Zahraa, Riyadh/Saudi Arabia The influence of phosphorus on the activity of organometallic "derived cluster" platinum catalysts	87— 88	43
J. R. Budge, B. F. Lücke, J. P. Scott, B. C. Gates, Newark DE/USA Alumina-supported CO hydrogenation catalysts derived from molecular RuOs ₃ , Ru ₄ and Os ₃ clusters	89— 96	43

Active phase-support interactions

M. A. Vannice, P. Chou, University Park, PA/USA The influence of the pretreatment and the support on benzene hydrogenation over palladium	99—110	27
J. B. F. Anderson, J. D. Bracey, R. Burch, A. R. Flambard, Whiteknights, Reading/UK Enhanced activity of titania-supported catalysts in the absence of strong metal-support interactions (SMSI)	111—121	27
D. C. Koningsberger, H. F. J. van't Blik, J. B. A. D. van Zon, R. Prins, Eindhoven/NL An EXAFS study of the influence of CO chemisorption on the structure of highly dispersed Rh/TiO ₂ catalysts	123—134	27

	Volume V Page	Programme Page
G. L. Haller, V. E. Henrich, M. McMillan, D. E. Resasco, H. R. Sadeghi, S. Sakellson, New Haven, CT/USA Geometric and electronic effects of SMSI in group VIII-TiO ₂ systems	135—145	27
Xie Youchang, Gui Linlin, Liu Yingjun, Zhao Biying, Yang Naifang, Zhang Yufen, Guo Qinlin, Duan Lianyun, Huang Huizhong, Cai Xiaohai, Tang Youchi, Peking/P.R. China Spontaneous monolayer dispersion of oxides and salts onto the surface of carriers and its application to heterogeneous catalysis	147—158	31
Y. Okamoto, Y. Konishi, K. Fukino, T. Imanaka, S. Teranishi, Osaka/J Metal-metal oxide interactions in Cu-ZnO catalysts for synthesis-gas reactions studied by X-ray photoelectron spectroscopy	159—170	31
Z. G. Szabó, T. Kovács, J. Juhász, E. Jover, Budapest/H, and Szazhalombatta/H Cadmium-oxide-sulfate — a promising multifunctional catalyst	171—182	31
I. Böszörményi, S. Dobos, L. Guczi, L. Markó, K. Lázár, W. M. Reiff, Z. Schay, L. Takács, A. Vizi-Orosz, Budapest/H, and Boston MA/USA Cluster-support interaction as a controlling factor in the formation of bimetallic catalysts	183—194	31
<u>Metal-support interactions</u>		
J. Goldwasser, C. Bolivar, C. Ramon Ruiz, B. Arenas, S. Wanke, H. Royo, R. Barrios, J. Giron, Caracas/YV and Edmonton/CDN Manifestations of metal support interactions in Pt/MgO for various reactions	195—204	44
Li Wenzhao, Chen Yixuan, Yu Chunying, Wang Xiangzhen, Hong Zupei, Wei Zhaobin, Dalian/P.R. China Studies on metal-semiconductor interaction over Pt/ZnO and Pt/TiO ₂	205—216	44
J. C. Conesa, P. Malet, A. Muñoz, G. Munuera, M. T. Sainz, J. Sanz, J. Soria, Madrid/E and Sevilla/E Effect of H ₂ on TiO ₂ -supported rhodium catalysts: spillover and SMSI	217—228	44
K.-H. Stadler, M. Schneider, K. Kochloeff, Munich/D Selective alkadiene hydrogenation over titania-supported palladium	229—238	44
J. A. Little, G. Butler, S. R. Daish, J. A. Tumbridge, Cambridge and Harwell/UK Microstructure and properties of an SMSI catalyst, nickel on mixed alumina/titania	239—250	44
K. Kunimori, H. Abe, E. Yamaguchi, S. Matsui, T. Uchijima, Ibaraki/J Strong metal-support interactions in Nb ₂ O ₅ -supported and TiO ₂ -supported metal catalysts: their effects on CO hydrogenation	251—262	44
C.-H. Yang, J. G. Goodwin, Jr., G. Marcelin, Pittsburgh PA/USA Additive effects of promotion and metal-support interactions on Fischer-Tropsch synthesis	263—273	44
R. Kramer, H. Zuegg, Innsbruck/A The hydrogenolysis of methylcyclopentane on platinum: influence of the support on the particle size effect	275—286	44
<u>Complex multicomponent catalysts</u>		
J. M. Dominguez E, D. R. Acosta N, Mexico/MEX Structural and compositional characterization of multiphase catalysts by AEM and TEM	287—298	44

Y. Inoue, K. Sato, S. Suzuki, I. Yoshioka, Niigata/J Polarization effects of LiNbO_3 ferroelectrics support upon adsorptive and catalytic properties of deposited Ag and NiO	299—310	44
M. A. Baltanas, A. B. Stiles, J. R. Katzer, Gent/B and Princeton NJ/USA Design of novel catalysts for partial oxidation: Catalytic and spectroscopic characterization of supported manganese oxides	311—321	44
N. Najbar, Kraków/PL Phase interaction in the evolution of the active mass of $\text{V}_2\text{O}_5\text{-MoO}_3$ catalyst for selective benzene oxidation	323—332	45
K. M. Abd El-Salaam, E. A. Hassan, A. A. Said, Assiut/Egypt Influence of foreign oxides added to unsupported V_2O_5 catalyst on its electronic properties during the thermal decomposition of 2-propanol	333	45
P. Putanov, R. M. Nedučin, G. Lomić, M. Genova, E. Kiš, Novi Sad/YU Mutual interdependent effects of the components in silica containing supported catalysts	335—346	45
F. Gopal, Teheran/IR On the catalytic properties of Al- and Cr-tungstates and some aspects of catalyst-support interactions	347	45
K. Soga, Y. Doi, T. Keii, Yokohama and Ooka/J The effect of magnesium chloride on the polymerization of α -olefins	349—358	45
V. N. Sapunov, N. N. Lebedev, I. Y. Litvinsev, V. D. Vardanian, Moscow/USSR Dependence of activity and selectivity of immobilized catalysts for hydroperoxide epoxidation of olefins on the structure of carrier	359—367	45

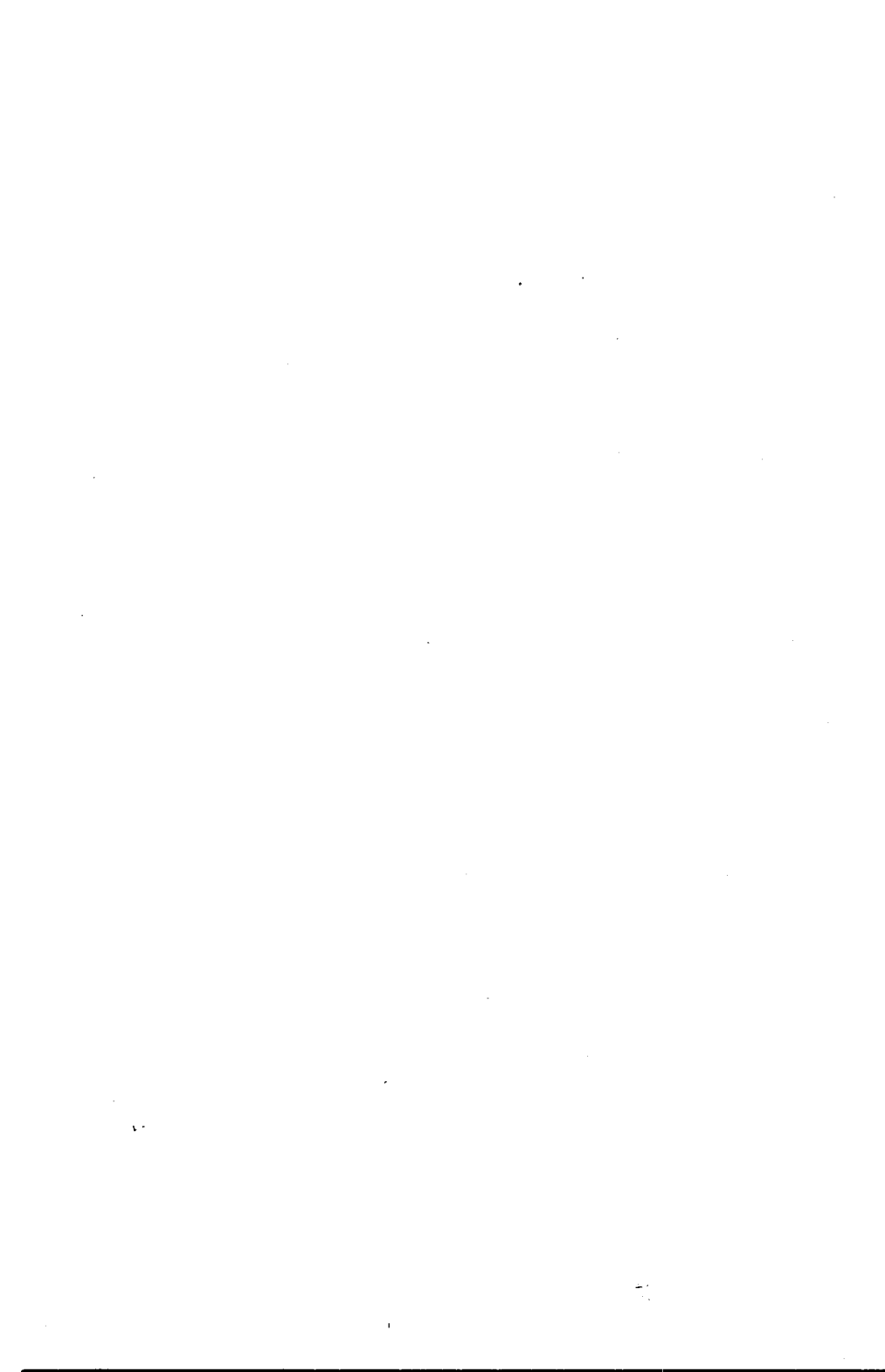
Catalysis for synthesis of chemicals

R. K. Grasselli, J. F. Brazdil, J. D. Burrington, Cleveland, OH/USA Solid state and surface mechanisms in selective oxidation and ammoxidation catalysis	369—380	25
A. Andersson, R. Wallenberg, S. T. Lundin, J.-O. Bovin, Lend/S An investigation of a mixed vanadium oxide catalyst in the ammoxidation of 3-picoline. TPO, TPD and HRTEM studies	381—392	25
P. J. van den Berg, K. van der Wiele, J. J. J. den Ridder, Delft/NL Selective oxidation and ammoxidation of aromatic hydrocarbons in the gas phase	393—403	25
Y. Ono, T. Baba, Tokyo/J The catalytic behavior of metal salts of heteropolyacids in the vapor-phase synthesis of methyl t-butyl ether	405—416	25
H. Bach, W. Gick, E. Wiebus, B. Cornils, Oberhausen-Holten/D Continuous hydroformylation with water-soluble Rh-catalysts	417—427	25
K.-Y. Zhou, Z.-X. Gao, W. Keim, Dalian/P.R. China, and Aachen/D Linear oligomerization of propylene with nickel complex catalysts	429—439	25
M. Bartók, Á. Molnár, I. Bucsi, Szeged/H Mechanism of configurational isomerization of 1,2-dimethylsilacyclopentanes on copper	441—452	25

	Volume V Page	Programme Page
N. Kitajima, J. Schwartz, Princeton, NJ/USA Metal-catalyzed selective chlorination of methane	453—461	25
<u>Heterogeneous gas phase oxidation</u>		
A. Baiker, P. Zollinger, Zürich/CH Structural dynamics of vanadium oxide catalyst in the oxidative ammonolysis of 3-picoline	463—474	46
M. Ai, Yokohama/J Partial oxidation of n-butane with heteropoly compound-based catalysts	475—486	46
M. Misono, N. Mizuno, T. Komaya, Tokyo/J Redox properties and oxidation catalysis of 12-molybdophosphates	487—498	46
K. Kürzinger, G. Emig, H. Hofmann, Hanau/D and Erlangen-Nürnberg/D Oxydehydrogenation of isobutyraldehyde and isobutyric acid as a new route to methacrylic acid	499—507	46
J. L. Herce-Vigil, J. Flores, M. Fraczak, R. Bugarel, Mexico/MEX Selective catalyst for some anhydride syntheses	509—518	46
R. Maggiore, S. Galvagno, G. Toscano, C. Crisafulli, A. Giannetto, J. C. J. Bart, Catania, Pistunina and Novara/I Allyl iodide transformation over molybdate catalysts	519—530	46
<u>Catalysis in the liquid phase</u>		
A. Tai, K. Tsukioka, Y. Imachi, Y. Inoue, H. Ozaki, T. Harada, Y. Izumi, Osaka and Tokyo/J Asymmetrically modified nickel catalyst (MNI) embedded in silicone polymer	531—542	46
E. I. Klabunovskii, A. A. Vedenyapin, B. G. Chankvetadze, G. C. Areshidze, Moscow and Tbilisi/USSR Study of copper-nickel catalysts' behaviour in enantioselective hydrogenation	543—552	46
A. O. I. Krause, L. G. Hammarström, M. Joutsimo, Kulloo/SF Etherification of C ₆ -olefins with methanol	553—563	46
A. Behr, K.-D. Juszak, R. He, Aachen/D Transition metal catalysed conversions of carbon dioxide with unsaturated compounds	565—572	46
T. Bartik, P. Heimbach, Essen and Mülheim-Ruhr/D Experimental methods to control metal-induced and metal-catalyzed organic synthesis	573—577	46
<u>Miscellaneous reactions</u>		
T. Yamaguchi, S. Nakamura, H. Nagumo, Sapporo/J Catalysis by supported tungsten oxide: a homologation reaction of ethylene in presence of hydrogen	579—590	47
A. H. Weiss, S. LeViness, V. Nair, L. Guzzi, A. Sarkany, Z. Schay, Worcester MA/USA and Budapest/H The effect of Pd dispersion in acetylene selective hydrogenation	591—600	47
K. Tanabe, T. Yamaguchi, K. Akiyama, A. Mitoh, K. Iwabuchi, K. Isogai, Sapporo and Shizuoka-ken/J The catalytic synthesis of acylated compounds by using solid super acid	601—610	47

	Volume V Page	Programme Page
J. G. Highfield, B. K. Hodnett, J. B. McMonagie, J. B. Moffat, Waterloo/CND The physical, structural and surface chemistry of heteropoly compounds and their relationship to catalytic properties	611—622	47
E. Echigoya, H. Sano, M. Tanaka, Tokyo/J Nature of active sites of acidic solid catalysts for the oxidative dehydrogenation of ethylbenzene	623—633	47
K. Deller, E. Koberstein, Hanau/D Catalytic investigations on the partial hydrogenation of glycolnitrile to glycolaldehyde	635—646	47
<u>Catalysis with zeolites and layered silicates</u>		
Y. Kitayama, T. Hoshina, T. Kimura, T. Asakawa, Ikarashi, Niigata/J Catalytic conversion from ethanol into butadiene by metal supported on clay minerals of sepiolite and attapulgite	647—657	47
G. Bergeret, P. Gallezot, Villeurbanne/F Modifications of the atomic structure of platinum aggregates in the course of n-butane conversion	659—666	22
K.-J. Chao, L.-J. Huarng, Hsinchu/Taiwan A study of mechanism of methanol conversion to hydrocarbons on ZSM-5	667—677	47
Y. Morikawa, K. Takagi, Y. Moro-oka, T. Ikawa, Yokohama/J Dehydrogenation of methanol to form methyl formate over cupric ion exchanged form of fluoro tetrasilicic mica	679—690	47
H. Bock, M. Haun, J. Mintzer, Frankfurt am Main/D The heterogeneously catalyzed gas phase reaction of olefins with water	691—699	47
Author Index	A-1 — A-19	

Cluster - derived catalysts



Study of Supported Rhodium Catalysts for Synthesis of Low Alcohols from CO and H₂

V.L. Kuznetsov, A.V. Romanenko, I.L. Mudrakovskii, V.M. Matikhin, V.A. Shmachkov, Yu.I. Yermakov, Institute of Catalysis, Novosibirsk 630090, USSR

Summary

The state of rhodium in the supported catalysts prepared via the adsorption of Rh₄(CO)₁₂ on SiO₂, γ-Al₂O₃ and La₂O₃ was investigated by XPS, EXAFS and IR spectroscopy, TPD and TPR. The existence of "pill-box" shape of rhodium particles on La₂O₃ and a decrease of heat of CO desorption in comparison with Rh/SiO₂ and Rh/Al₂O₃ catalysts were indicative of strong metal support interaction (SMSI) of Rh with La₂O₃. The high yield of oxygenated products at CO hydrogenation was characteristic for Rh/La₂O₃ catalysts. ¹³C-NMR studies suggest that the interaction of CO and H₂ over Rh/La₂O₃ initially produces species containing $\begin{array}{c} \text{O} \\ \parallel \\ \text{C} \\ \diagup \text{H} \end{array}$ fragments. Formation of CHO₂⁻ species is also probable. Experimental data are obtained showing that methanol and ethanol formation proceeds through different mechanisms involving different catalytic sites.

At CO hydrogenation by Rh containing catalysts it is possible to obtain either hydrocarbons or oxygenated compounds /1-3/(especially it is necessary to mention the formation of C₂ oxygenates /4,5/). The state of Rh in these catalysts is a problem under discussion /2,3,5, 6/. Some important features of the mechanism of CO hydrogenation on Rh catalysts are also not clear. Methanol is suggested to be formed through the hydrogenation of non-dissociatively adsorbed CO. This view is compatible with the results of isotopic mixing technique for Rh/TiO₂ /7/. But the type and the location of catalytic sites responsible for the methanol formation however are not known. It was proposed that hydrocarbons and C₂-oxygenates are formed via a common CH_x precursor /1,2,6,8/. However, it is not clear if these species are derived from dissociatively adsorbed CO with subsequent hydrogenation of surface carbon or from non-dissociatively adsorbed CO by its direct hydrogenation.

The present paper reports the results of the study of Rh catalysts characterized by different selectivities in CO hydrogenation. This study was performed with an objective to clarify the state of Rh in

these catalysts and the mechanism of alcohols formation.

Experimental

Rhodium catalysts were prepared via the impregnation of oxide supports preliminary heated at 573-873 K in vacuum with pentane solution of $\text{Rh}_4(\text{CO})_{12}$. After evacuation of the solvent supported clusters were decomposed at 423-443 K in vacuum. All the procedures of preparation and treatment of catalysts were carried out without the exposure in air. Some characteristics of the catalysts prepared are given in table 1.

Table 1

Properties of rhodium catalysts prepared by supporting $\text{Rh}_4(\text{CO})_{12}$
Rhodium content ~1 wt%.

Support	T_d, K^a	B.E.T. surface area m^2/g	T_r in H_2, K	$\frac{H}{Rh}^b$	$\frac{CO}{Rh}^b$	$\bar{d}_{e.m.}^c$ nm	E_b and E_d halfwidth of $Rh\ 3d_{5/2}$ line eV
SiO_2	873	200	673	0.7	0.6	3.7	306.8(2.0)
$\gamma-Al_2O_3$	873	220	673	1.6	2.1	≤ 1.0	307.7(2.2)
La_2O_3 ^e	573	33	473	0.6	0.9	-	307.3(3.5)
			673	1.15	0.4	-	307.1(2.9)
			873	0.6	0.2	-	307.1(2.2)
$La-SiO_2$ ^f (10 wt% La)	773	180	473	1.7	1.7	2.0^g	-
			673	1.9	2.0	2.0^g	-
			873	1.4	1.6	2.0^g	-

a - Temperature of preheating of support; b - measured in Digisorb-2500 at 298 K; c - average diameter of rhodium particles, electron microscopic data; d - XPS data; e - prepared according to ref. 9; f - prepared via impregnation of SiO_2 with water solution of $La(OOCCH_3)_3$ and subsequent heating of the support in vacuum at 773 K; g - "pill-box" particles.

XPS studies were carried out using VG-ESCA-3 spectrometer with Al K radiation. The Si 2p (103.7 eV), Al 2p (74.7 eV) and C 1s (284.8 eV) lines were used as internal standards. Electron microscopic

measurements were performed using EMV-100B electron microscope with 0.3 nm resolution. EXAFS K-spectra of rhodium were recorded using synchrotron radiation facilities of the Institute of Nuclear Physics (Novosibirsk). IR spectra of CO adsorbed on catalysts were recorded using Specord 75 IR in a cell providing possibility to treat the wafer of a catalyst without contact with air. TPD of CO and H₂ were carried out in a vacuum system (5×10^{-6} Pa) with a linear heating (5 K/min). The temperature programmed reduction (TPR) of initially oxidized Rh catalysts were studied in the installation by the same technique as described in ref. 10 (7 vol.% H₂ in Ar, space velocity 200-400 min⁻¹, heating 11 K/min). ¹³C-NMR spectra were registered using CXP-300 spectrometer (Bruker) at the constant magnetic field of 7T and frequency of 75.5 MHz. Measurements of activity of CO hydrogenation were carried out at atmospheric pressure in a glass flow differential reactor at 473-573 K and space velocity of the CO and H₂ mixture (1:2) of 500-80000 hr⁻¹. The products were analyzed chromatographically.

Results

Catalytic properties of rhodium catalysts

Table 2 summarizes the properties of rhodium catalysts in CO hydrogenation. The yield of oxygenated compounds (methanol, ethanol and traces of acetaldehyde) significantly depends on the space velocity of CO and H₂ mixture (alcohols may be decomposed in the secondary reactions; the rate of methanol formation also decreases with an increase of conversion). So catalytic properties of different samples were compared at the same space velocities. The Rh/La₂O₃ and Rh/La-SiO₂ show a higher yield of methanol and ethanol, which accounts for that these catalysts were studied in more detail.

An increase of the temperature of preliminary reduction of Rh/La₂O₃ in H₂ resulted in an increase of the relative yield of ethanol and a decrease of the yield of methanol (fig. 1). The introduction of O₂ in the reaction mixture (CO:H₂:O₂=1:2:0.002) resulted in a decrease of the activity of rhodium catalysts.

An addition of CH₃OH in CO and H₂ mixture (40% of CO converted) didn't change significantly the yields of oxygenated products in the case of Rh/La₂O₃. However, the addition of CH₃I (20-30% of CO converted; the

Table 2

Catalytic properties of supported rhodium catalysts in CO hydrogenation (CO:H₂=1:2; 523 K; 10 hours after the beginning of catalytic tests).

Catalyst	Space velocity h ⁻¹	Carbon efficiency ^a				rate of formation A _i × 10 ⁵		
		hydrocarbons		CH ₃ OH	C ₂ H ₅ OH			
		C ₁	C ₂ -C ₅			CH ₄	CH ₃ OH	C ₂ H ₅ OH
Rh/SiO ₂	2700	43.8	56.2	+	+	393.0	+	+
Rh/Al ₂ O ₃ ^b	1800	42.8	57.2	+	+	11.0	+	+
Rh/La ₂ O ₃	3200	43.2	12.5	27.1	17.2	21.5	13.5	4.3
							(44.5) ^c	
	11000	29.7	7.9	36.6	25.8	25.1	31.0	11.0
							(102.2) ^c	
Rh/La-SiO ₂	3200	71.8	10.8	8.5	8.9	83.4	9.9	5.2
	16500	61.2	10.2	17.4	11.2	106.0	30.2	9.1
La ₂ O ₃	3600	-	-	100	-	-	-(3.0) ^c	-

a Carbon efficiency = $(n_i A_i / \sum n_i A_i) \times 100$; n_i - number of carbon atoms in product i ; A_i = (mol product i × g-at Rh⁻¹ × s⁻¹); b prepared by reduction of RhCl₃/Al₂O₃ at 723 K in H₂; c rate of methanol formation calculated per 1 m² of La₂O₃ mol CH₃OH × (m² La₂O₃ × s)⁻¹ × 10¹¹.

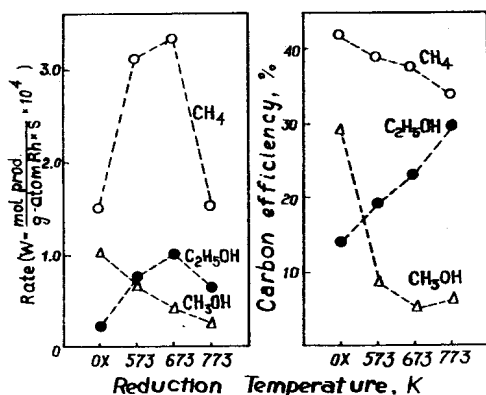


fig. 1

Effect of the temperature of Rh/La₂O₃ reduction on the yield of CO and H₂ reaction products (523 K, CO:H₂=1:2; 3250 hr⁻¹). "0x" stands for Rh₄(CO)₁₂/La₂O₃ sample oxidized in air at 293 K (reduction in the reaction conditions).

consumption of CH_3I reached 85-98%) led to a drastic decrease of methanol yield, whereas the yield of ethanol somewhat increased (20-25%). When the addition of CH_3I was stopped the yield of ethanol decreased till the value characteristic for $\text{Rh}/\text{La}_2\text{O}_3$ in the absence of CH_3I . The rate of methanol formation was still very low.

State of Rh in catalysts

TFR. Hydrogen consumption by oxidized rhodium catalysts was observed at the temperature above 373 K (fig. 2). For $\text{Rh}/\text{La}_2\text{O}_3$ the consumption of H_2 ($\text{H}:\text{Rh}=25-30$) was much higher than it is necessary for a 3-electron reduction of Rh^{3+} . In this case the formation of methane was observed; the amount of CH_4 (0.1 mol $\text{CH}_4/\text{g-atom La}$) was compatible with the amount of hydrogen consumed (0.25 mol $\text{H}_2/\text{g-atom La}$). CH_4 may originate from the hydrogenation of surface carbonate groups of La_2O_3 by the hydrogen activated on Rh.

XPS data. The values of binding energies of the Rh $3d_{5/2}$ level are presented in table 1. These values for Rh/SiO_2 and $\text{Rh}/\text{La}_2\text{O}_3$ catalysts were close to those typical for metallic rhodium (307.0±1 eV). For $\text{Rh}/\text{La}_2\text{O}_3$ the Rh $3d_{5/2}$ line was however somewhat broader. In the case

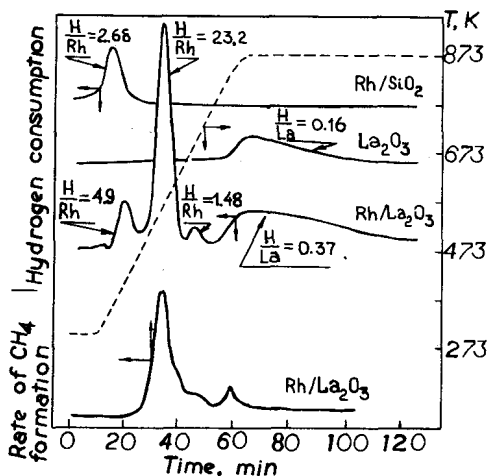


fig. 2

TPR spectra for Rh/SiO_2 , La_2O_3 , $\text{Rh}/\text{La}_2\text{O}_3$, $\text{Rh}_4(\text{CO})_{12}/\text{SiO}_2$ and $\text{Rh}_4(\text{CO})_{12}/\text{La}_2\text{O}_3$ were used for TPR experiments after their oxidation in air.

of $\text{Rh}/\text{Al}_2\text{O}_3$ a significant shift of $\text{Rh } 3d_{5/2}$ line towards higher bond energies was observed.

Fourier transforms of EXAFS K-spectra of rhodium catalyst with assignment of peaks /11/ are given in fig. 3. For marked peaks the specification of types of atoms and distances was carried out by using the nonlinear least squares fitting method. In the case of $\text{Rh}/\text{La}_2\text{O}_3$ and $\text{Rh}/\text{La}-\text{SiO}_2$ (reduced at 773 K) the portion of rhodium atoms which have direct contact with oxygen atoms of the support ($r_0 - \delta = 0.18$ and 0.2 nm) is greater than for Rh/SiO_2 and $\text{Rh}/\text{Al}_2\text{O}_3$. It corresponds to the presence of "pill-box" shape particles of rhodium on the surface of La_2O_3 and $\text{La}-\text{SiO}_2$. Electron microscopic pictures of $\text{Rh}/\text{La}-\text{SiO}_2$ show the presence of semitransparent particles less than 2.0 nm /11/.

An increase in the reduction temperature of $\text{Rh}/\text{La}-\text{SiO}_2$ up to 873 K didn't influence the size of rhodium particles. At the same time in the radial structure function (fig. 3) diminishing of peak of the second coordination shell of rhodium in metal particles ($\text{Rh}-\text{Rh}^2$) and shortening of the distance of the first coordination shell of rhodium ($\text{Rh}-\text{Rh}^1$) were observed. Such changes in the radial structure function corresponded to the strengthening of the interaction of rhodium with the support. In the case of $\text{Rh}/\text{Al}_2\text{O}_3$ peak (0.16 nm) corresponding to the distance $\text{Rh}-\text{O}$ in Rh_2O_3 was observed.

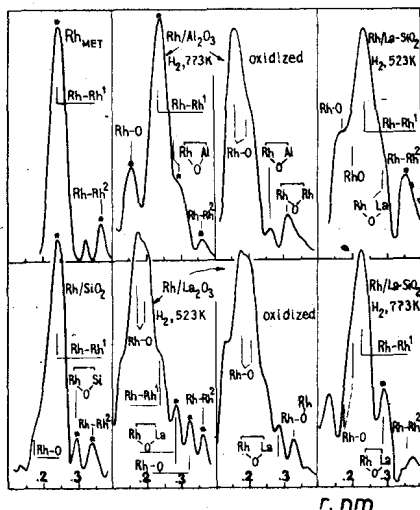


fig. 3

Fourier transforms of EXAFS K-spectra of rhodium catalysts. $\text{Rh}/\text{Al}_2\text{O}_3(\text{ox})$ and $\text{Rh}/\text{La}_2\text{O}_3(\text{ox})$ were used after the oxidation of $\text{Rh}_6(\text{CO})_{16}/\text{Al}_2\text{O}_3$ and $\text{Rh}_4(\text{CO})_{12}/\text{La}_2\text{O}_3$ respectively in air at 298 K. ($\text{Rh}-\text{Rh}^1$ and $\text{Rh}-\text{Rh}^2$ stand for the distances in the first and the second coordination shells of metallic rhodium particles). $r = r_0 - \delta$ is the distance without taking into account the phase shift (δ); r_0 is the true distance.

IR spectra. CO adsorption on Rh/SiO_2 , $\text{Rh}/\text{La}_2\text{O}_3$ and $\text{Rh}/\text{La}-\text{SiO}_2$ after their treatment by CO and H_2 at 523 K led to the appearance of two types of bands corresponding to linear (I; $2040-2065\text{ cm}^{-1}$) and bridged (II; $1850-1870\text{ cm}^{-1}$) CO groups coordinated on metallic rhodium. In the case of $\text{Rh}/\text{Al}_2\text{O}_3$ twin bands (type III) 2090 and 2015 cm^{-1} along with the bands of CO adsorbed on metallic rhodium were observed. Bands of type III were attributed to symmetric and antisymmetric vibrations of CO groups ($\text{Rh}(\text{CO})_2$) coordinated by ions of $\text{Rh}(\text{I})/12,13/$ or atoms of two dimensional particles of metal $/6,14/$. Treatment of Rh/SiO_2 , $\text{Rh}/\text{La}_2\text{O}_3$ and $\text{Rh}/\text{La}-\text{SiO}_2$ at $298-373\text{ K}$ by O_2 resulted in the appearance of CO bands of type III. However, in the conditions of CO hydrogenation the bands of type III quickly ($1-20\text{ min}$) disappeared and only bands of type I and II were observed.

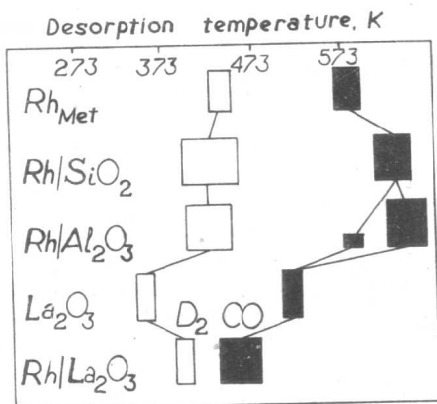


fig. 4

Temperatures of the maximum desorption rate of CO and D_2 from rhodium catalysts.

This corresponds to diminishing of the desorption heat of CO by $40-65\text{ kJ/mol}$ $/15/$.

^{13}C NMR was used for study of surface species formed as a result of CO and H_2 interaction on La_2O_3 , $\text{Rh}/\text{La}_2\text{O}_3$ and Rh/SiO_2 . ^{13}C NMR spectra obtained for SiO_2 and Rh/SiO_2 were characterized by far lower intensity than those for La_2O_3 and $\text{Rh}/\text{La}_2\text{O}_3$. We observed no CO groups chemisorbed on Rh particles due to low concentration of Rh. The spectrum of CO adsorbed on SiO_2 exhibits a single line with $\delta = 184\text{ ppm}$ and

Data on TPD of CO and D_2 from Rh catalysts are summarized in fig. 4. We used a low heating rate to provide a uniform heating of catalysts. But because of a possible readorption of gases it was difficult to calculate the accurate values of desorption heats $/15/$. However, comparison of relative positions of TPD peaks gives possibility to estimate the difference between values of desorption heats of gases from catalysts. The maximum of desorption rate of CO from $\text{Rh}/\text{La}_2\text{O}_3$ shifted significantly to lower temperatures in comparison with those typical for metallic rhodium, Rh/SiO_2 and $\text{Rh}/\text{Al}_2\text{O}_3$.